Difference in metabolite levels between photoautotrophic and photomixotrophic cultures of *Synechocystis* sp. PCC 6803 examined by capillary electrophoresis electrospray ionization mass spectrometry

Hideyuki Takahashi[1], Hirofumi Uchimiya[1,2] and Yukako Hihara[3,*]

[1] Institute of Molecular and Cellular Biosciences, The University of Tokyo, 1-1-1 Yayoi, Bunkyo-ku, Tokyo 113-0032, Japan

[2] Iwate Biotechnology Research Center, Kitakami, Iwate 024-0003, Japan

[3] Department of Biochemistry and Molecular Biology, Faculty of Science, Saitama University, Shimo-okubo, Saitama, 333-8570, Japan

* Corresponding author:

Department of Biochemistry and Molecular Biology, Faculty of Science, Saitama University, 255 Shimo-okubo, Sakura-ku, Saitama 338-8570, Japan

Tel: +81-48-858-3396, Fax: +81-48-858-3384, E-mail: hihara@molbiol.saitama-u.ac.jp

The data of submission: May 3, 2008, Number of tables: 0, Number of figures: 7

Running title: metabolome of photomixotrophically grown cyanobacteria

key words: CE/MS, cyanobacteria, glucose, *pmgA*, metabolome, photomixotrophy

Abbreviations: CE/MS, Capillary electrophoresis mass spectrometry; DHAP, dihydroxyacetone phosphate; FBP, fructose-1,6-bisphosphate; GA3P, glyceraldehyde-3-phosphate; GAPDH, glyceraldehyde-3-phosphate dehydrogenase; G6P, glucose-6-phosphate; G6PDH, glucose-6-phosphate dehydrogenase; ICDH, isocitrate dehydrogenase; 2-OG, 2-oxoglutarate; OPP pathway, oxidative pentose phosphate pathway; PEP, phospho*enol*pyruvate; 3PGA, 3-phosphoglycerate; 6PG, 6-phosphogluconate; 6PGDH, 6-phosphogluconate dehydrogenase; PRK, phosphoribulokinase; R5P, ribose-5-phosphate; Ru5P, ribulose-5-phosphate; RuBP, ribulose-1,5-diphosphate; TCA cycle, tricarboxylic acid cycle.

Abstract

Capillary electrophoresis mass spectrometry (CE/MS) was applied for the comprehensive survey of changes in the amounts of metabolites upon the shift from photoautotrophic to photomixotrophic conditions in *Synechocystis* sp. PCC 6803. When glucose was added to the photoautotrophically grown culture, the increase of the metabolites for oxidative pentose phosphate pathway and glycolysis together with the decrease of those for the Calvin cycle was observed. Concomitantly, the increase of respiratory activity and the decrease of photosynthetic activity took place in the wild-type cells. In *pmgA*-disrupted mutant that shows growth inhibition under photomixotrophic conditions, lower enzymatic activities of the oxidative pentose phosphate pathway and higher photosynthetic activity were observed irrespective of trophic conditions. These defects brought about metabolic disorders such as the decrease in ATP and NADPH contents, failure in activation of respiratory activity and aberrant accumulation of isocitrate under photomixotrophic but not under photoautotrophic conditions. A delicate balancing of the carbon flow between the Calvin cycle and the OPP pathway seems indispensable for growth specifically under photomixotrophic conditions and PmgA is likely to be involved in the regulation.

Introduction

Photosynthetic organisms face continuous constrains in their growth environment. In order to meet the energy demands for sustainable life, cyanobacteria show versatile growth characteristics in response to the availability of light and carbon source (Rippka *et al*., 1979; Stal and Moezelaar, 1997). They are primarily photoautotrophic organisms performing oxygenic photosynthesis to convert the light energy to the chemical energy. ATP and NADPH generated by photosynthesis are used for assimilation of CO_2 by the Calvin cycle and the excess carbon fixed is stored in the form of glycogen. Some cyanobacterial species have ability of heterotrophic energy generation in addition to the photosynthetic capability: they catabolize glucose via the oxidative pentose phosphate (OPP) pathway, the glycolytic pathway, and an incomplete tricarboxylic acid (TCA) cycle to produce ATP, NADPH and carbon skeletons used as anabolic precursors. In cyanobacteria having no organelle, all of above mentioned metabolisms, CO_2 fixation, gluconeogenesis and glycolysis, are performed in cytoplasm and several enzymes are shared among these pathways (Smith, 1982). Thus, the control of functionally equivalent reactions in anabolic and catabolic pathways seems prerequisite for optimized growth under different trophic conditions.

The alteration in the metabolic processes in response to the environmental

change has been examined using a glucose-tolerant strain of *Synechocystis* sp. PCC 6803 that is capable of photoautotrophic, photomixotrophic and heterotrophic growth. The availability of light energy significantly affects the expression level of mRNA (Gill *et al*., 2002), that of proteins (Yang *et al*., 2002*a*; Kurian *et al*., 2006) and cellular metabolism (Yang *et al*., 2002*a*) in *Synechocystis*. When cultures are transferred from photoautotrophic to dark heterotrophic conditions with glucose, CO_2 assimilation by the Calvin cycle is rapidly inactivated and the major metabolic pathway switches from the Calvin cycle to the OPP pathway (Pelroy *et al*., 1972). On the other hand, the addition of glucose in the presence of light, namely, the shift from photoautotrophic to photomixotrophic conditions, hardly affects expression pattern of transcripts (Yang *et al*., 2002*a*; Kahlon *et al*., 2006) and of proteins (Yang *et al*., 2002*a*; Herranen *et al*., 2004). Under photomixotrophic conditions where both light and glucose are available, substantial activity of the Calvin cycle is detected (Yang *et al*., 2002*a*, 2002*b,* 2002*c*). Early works showed that the OPP pathway is repressed in the presence of light through the allosteric inhibition of glucose-6-phosphate dehydrogenase (G6PDH) by ribulose-1,5-diphosphate (RuBP), an intermediate of the Calvin cycle (Pelroy *et al*., 1972). Thus, the metabolic characteristic of photomixotrophic cultures has been considered to be similar to that of photoautotrophic ones: it is largely dependent on

photosynthesis but not on glucose catabolism. However, recent studies reported the detection of high G6PDH activity in photomixotrophically grown cells (Knowles and Plaxton, 2003; Singh and Sherman, 2005; Kahlon *et al*., 2006). This implies that both the Calvin cycle and the OPP pathway, whose enzymatic reactions proceed in the reverse direction for the most part, can coexist under photomixotrophic conditions. If this is the case, there must be a regulatory mechanism to coordinate anabolic and catabolic activities upon the shift from photoautotrophic- to photomixotrophic conditions. At present, information on such a regulatory mechanism is not available, since there is no comprehensive study focused on the difference in metabolic processes under these two trophic conditions.

In this study, we employed two strategies to address the mechanism that enables *Synechocystis* sp. PCC 6803 to grow photomixotrophically. First, capillary electrophoresis mass spectrometry (CE/MS) was applied for the comprehensive survey of metabolic processes, since this method is useful for simultaneous detection of metabolites, especially charged ones such as organic acids and nucleotides. In previous reports, the CE/MS method successfully revealed metabolite alterations in *Bacillus subtilis* (Soga *et al*., 2002), *Oryza sativa* (Sato *et al*., 2004; Takahashi *et al*., 2006*a*) and *Arabidopsis thaliana* (Takahashi *et al*., 2006*b*). Second, to unravel the regulatory

mechanism required for photomixotrophic growth, we compared amounts of metabolites between the wild-type and a mutant showing sensitivity to photomixotrophic conditions. The gene-disrupted mutant of *pmgA* (sll1968) encoding a putative regulatory protein can grow normally under photoautotrophic or heterotrophic condition but suffers severe growth inhibition under photomixotrophic condition (Hihara and Ikeuchi, 1997). Metabolic characterization of such a regulatory mutant showing light/glucose sensitivity seems a good approach to clarify regulatory processes required for photomixotrophic growth.

Materials and Methods

Strains and culture conditions

A glucose-tolerant wild-type strain of *Synechocystis* sp. PCC 6803 and the *pmgA*-disrupted mutant made by inserting the spectinomycin resistance cassette (Hihara and Ikeuchi, 1997) were used for the study. They were grown at 32˚C in BG-11 medium with 20 mM HEPES-NaOH, pH 7.0, under continuous illumination of 50 μmol photons m^{-2} s^{-1}. Cultures were grown in volumes of 50 ml in test tubes (3 cm in diameter) and bubbled by air supplemented with 1% CO_2. Cell density was estimated at A_{730} using a

spectrophotometer (model UV-160A, Shimadzu, Kyoto, Japan). For the comparison of photomixotrophic culture with photoautotrophic one, photoautotrophically grown cultures at mid log phase were inoculated into the fresh medium with or without 5 mM glucose at A_{730} = 0.05 - 0.1 and incubated at 50 μmol photons m^{-2} s^{-1} for the indicated duration.

Metabolite analysis

Quantification of metabolites was performed by the method described by Takahashi *et al*. (2006*b*). Fifty ml of cultures were harvested by centrifugation at 15,000 x g at 4°C for 2 min and the obtained cell pellets (30-50 mg in fresh weight) were frozen in liquid nitrogen. Samples were vortexed with 200 μl of ice-cooled 50% (v/v) methanol containing internal standards (50 μM PIPES) for 10 min. The supernatant was recovered by centrifugation at 15,000 x g at 4°C for 5 min, filtered with a 5-kDa-cutoff filter (Millipore, Bedford, MA, USA), and used for analysis by CE/MS. Separation of metabolites was performed on a polyethylene glycol-coated capillary (DB-WAX, 100 cm×50 μm I.D., J&W Scientific, Folsom, CA, USA) using 20 mM ammonium acetate, pH 6.8, as a running buffer. Metabolites in the extract were identified by comparison of the migration time and m/z ratio with those of authentic organic acids and nucleotides.

The quantification was performed by comparing peak areas of metabolites in samples with those of the authentic standards. As for glyceraldehyde-3-phosphate (GA3P) that exists as both the labile diol and the stable aldehyde forms in aqueous solution (Trentham *et al*., 1969), the stable form was specifically detected by CE/MS.

Measurement of enzymatic activities of cells

Fifty ml of cultures were harvested by brief centrifugation and resuspended with 500 μl of 50 mM sodium phosphate buffer, pH 7.5, containing 3 mM $MgCl_2$ and 1 mM DTT. Approximately 250 μl volume of zircon beads (0.1 mm in diameter, Biospec, Bartlesville, OK, USA) were added to the cell suspension and the cells were broken by four times of vigorous vortexing for 2 min followed by cooling on ice for 1 min. The lysate was centrifuged at 15,000 x g for 10 min and the resulting supernatant was used for the measurement.

$NADP^+$- specific enzymatic activities in cell extracts were measured spectrophotometrically by monitoring the substrate-dependent generation of NADPH at 340 nm. For measurements of the activities of glucose-6-phosphate dehydrogenase (G6PDH), 6-phosphogluconate dehydrogenase (6PGDH) and isocitrate dehydrogenase (ICDH), the reaction mixture containing 100 mM sodium phosphate buffer, pH 7.5, 3

mM $MgCl_2$, 0.4 mM $NADP^+$ and the cell extract in a total volume of 1 ml was used. For measurements of aconitase activity, the reaction mixture containing 100 mM sodium phosphate buffer, pH 7.5, 15 mM $MgCl_2$, 1 mM $NADP^+$, 1 mM EDTA, the cell extract and $NADP^+$-dependent ICDH (0.6 units) in a total volume of 1 ml was used. Reactions were started by the addition of respective substrates at 30ºC. Five mM glucose-6-phosphate, 5 mM 6-phosphogluconate, 2.5 mM isocitrate and 30 mM *cis*-aconitate were added as substrates for the measurements of G6PDH, 6PGDH, ICDH and aconitase, respectively. 1 U of enzymatic activity corresponds to the formation of 1 μmol NADPH/min under standard assay conditions.

Protein concentration was determined using Protein Assay Kits II (Bio-Rad Laboratories, Hercules, CA, USA) according to manufacturer's instructions.

Measurement of photosynthetic and respiratory activities of cells

An aliquot (1 ml) of photoautotrophically- or photomixotrophically- grown cultures was placed in a Clark-type oxygen electrode chamber and stirred gently at 30ºC. Whole-cell photosynthetic activity was measured as oxygen evolution supported by 2 mM $NaHCO_3$ at 50 μmol photons m^{-2} s^{-1}. Respiratory activity was measured as oxygen consumption in the presence of 5 mM glucose in the dark. The rates of oxygen

evolution and consumption were calculated in terms of μmol of oxygen evolved (10^8 cells)$^{-1}$ h^{-1} and of μmol of oxygen consumed (10^8 cells)$^{-1}$ h^{-1}, respectively.

Results

Growth properties of the wild-type and pmgA-disrupted mutant cells under photomixotrophic condition

First, we examined the growth properties of the wild-type cells and *pmgA*-disrupted mutant (Δ*pmgA* mutant) under photomixotrophic conditions (Fig. 1). Five mM glucose was added to the photoautotrophically grown cultures at time 0. When the cultures were diluted every 24 h to minimize the self-shading effect, the delay of the growth in Δ*pmgA* mutant became prominent in the second day. The growth of the mutant completely stopped in the third day, whereas the wild-type cells did not suffer any growth inhibition. If the mutant has any defects in the regulation of metabolic processes, aberrant levels of metabolites should be detected preceding the growth inhibition. Thus, we decided to examine the amounts of metabolites in cultures incubated under photomixotrophic conditions for 24 h.

Amounts of metabolites in glycolysis, the OPP pathway and the Calvin cycle

The amounts of metabolites engaged in the central carbon metabolic pathway in cyanobacteria (Fig. 2) were examined using CE/MS. Figure 3 shows the amounts of metabolites in glycolysis, the OPP pathway and the Calvin cycle in the wild-type and Δ*pmgA* mutant cells incubated under photoautotrophic or photomixotrophic conditions for 24 h. The presence of glucose had a great impact on the amounts of these metabolites in both strains. Namely, the levels of glucose-6-phosphate (G6P), fructose-1,6-bisphosphate (FBP), dihydroxyacetone phosphate (DHAP), glyceraldehyde-3-phosphate (GA3P), 6-phosphogluconate (6PG), ribose-5-phosphate (R5P), and ribulose-5-phosphate (Ru5P) increased significantly, while those of RuBP, 3-phosphoglycerate (3PGA), phospho*enol*pyruvate (PEP) and pyruvate showed marked decrease. It is notable that GA3P, 6PG, Ru5P, and RuBP contents were lower in the mutant than in the wild-type under photomixotrophic conditions.

Amounts of metabolites in the TCA cycle

Next, contents of metabolites related to the TCA cycle were examined (Fig. 4A). Incubation under photomixotrophic conditions led to the increase in contents of malate, fumarate, and isocitrate, while succinate and 2-oxoglutarate (2-OG) contents

decreased in both strains. Surprisingly, isocitrate content in Δ*pmgA* mutant increased up to 10-fold by incubation with glucose, whereas that in the wild-type showed only a slight increase. Then, we examined the time course of isocitrate accumulation after the addition of glucose (Fig. 4B). In the wild-type cells, isocitrate content was slightly increased, while it showed approximately 10-fold increase within 6 h in the mutant and stayed almost constant level until 24 h after glucose addition.

Amounts of adenine- and pyridine-nucleotides

The amounts of adenine- and pyridine-nucleotides were examined (Fig. 5). In the wild-type cells incubated with glucose for 24 h, the increase of NADH, AMP and ADP contents and the decrease of NAD^+, $NADP^+$ and NADPH contents were observed. In the case of Δ*pmgA* mutant under photoautotrophic conditions, nucleotide contents were almost the same as those in the wild-type cells except for the lower amount of NADPH. On the other hand, under photomixotrophic conditions, $NADP^+$, NADPH and ATP contents were significantly lower in the mutant. In both strains, ratio of NADH to total (NAD^++NADH) increased, whereas that of NADPH to total ($NADP^+$+NADPH) hardly changed upon the shift to photomixotrophic conditions.

Enzymatic activities

For better understanding of the changes in the metabolite levels, we examined the glucose-dependent change in enzymatic activities that are suspected to differ between the wild-type and Δ*pmgA* mutant cells. Cell extracts were prepared from cultures incubated under photomixotrophic conditions for 0, 1, 3, 6 and 24 h. Using this, first we determined the activities of glucose-6-phosphate dehydrogenase (G6PDH) and 6-phosphogluconate dehydrogenase (6PGDH) that control the carbon flow into the OPP pathway. As shown in Fig. 6, activities of these enzymes were only slightly affected by the addition of glucose. A notable finding is that these activities in the mutant were considerably lower than those in the wild-type cells irrespective of trophic conditions.

The aberrant accumulation of isocitrate in the mutant may be caused by the defect in the isocitrate formation catalyzed by aconitase and/or the degradation catalyzed by $NADP^+$-dependent isocitrate dehydrogenase (ICDH). Thus, we examined the time course change of the activity of these enzymes (Fig. 6). The aconitase activity was up-regulated within 1 h, whereas the ICDH activity was hardly affected by the addition of glucose. In both cases, no difference in the enzymatic activity was observed between the wild-type and Δ*pmgA* mutant. ICDH activity is dependent on the level of $NADP^+$ which was shown to be low in the mutant under photomixotrophic conditions

(Fig. 5). Thus, there is a possibility that *in vivo* activity of ICDH in the mutant is restricted by the availability of $NADP^+$, though such a limitation cannot be observed in the reaction mixture containing enough amount of $NADP^+$. To test this possibility, we examined the intracellular level of $NADP^+$ after 6 h of the addition of glucose where the accumulation of isocitrate became prominent in the mutant cells (Fig. 4B). At this time point, $NADP^+$ decreased by half of the initial level and there was no difference in the amount between two strains (not shown). This indicates that the activity of $NADP^+$-ICDH in the mutant is normally regulated also *in vivo*.

Photosynthetic and respiratory activities

We examined the photosynthetic and respiratory activities of the wild-type and Δ*pmgA* mutant cells incubated under photoautotrophic or photomixotrophic conditions for 24 h. Photosynthetic activity was measured as a rate of $NaHCO_3$-dependent oxygen evolution under the growth conditions, that is, at illumination of 50 μmol photons $m^{-2}s^{-1}$ with or without 5 mM glucose (Fig. 7A). In the wild-type cells, oxygen evolution rate decreased to two-thirds of the initial level upon the addition of glucose. Oxygen evolution rate of Δ*pmgA* mutant was higher than that of the wild-type under photoautotrophic conditions, which is consistent with the previous observation (Hihara

et al., 1998). Although oxygen evolution rate decreased also in the mutant after the addition of glucose, the resultant activity was still considerably higher than that in the wild-type. Respiratory activity was measured as a rate of oxygen consumption under dark conditions in the presence of 5 mM glucose (Fig. 7B). When incubated with glucose for 24 h, oxygen consumption rate increased 1.5-fold in the wild-type cells, whereas it hardly changed in Δ*pmgA* mutant.

Discussion

The difference in metabolic processes between photoautotrophically- and photomixotrophically-grown cultures of Synechocystis sp. PCC 6803

In this study, we showed that the level of metabolites in *Synechocystis* cells are significantly affected by the transfer from photoautotrophic to photomixotrophic conditions, irrespective of the almost unchanged levels of transcripts (Yang *et al*., 2002*a*; Kahlon *et al*., 2006) and of proteins (Yang *et al*., 2002*a*; Herranen *et al*., 2004). It is evident that metabolic balance is shifted toward catabolism by the addition of glucose, although anabolic pathways are still active unlike in the case of transfer to heterotrophic conditions.

After 24 h of incubation under photomixotrophic conditions, amounts of G6P, 6PG, Ru5P, R5P, FBP, GA3P and DHAP increased (Fig. 3), indicating the increase of carbon flow to the OPP pathway and glycolysis. In cyanobacteria, the major route of glucose catabolism was suggested to be the OPP pathway and the lower part of the glycolytic pathway (Pelroy *et al*., 1972), whereas the contribution of the upper part of the glycolytic pathway has been elusive. However, our results clearly show that both the OPP pathway and the whole part of glycolysis actively participate in glucose catabolism. The increase of NADH content under photomixotrophic conditions (Fig. 5) also indicates the enhanced flow through glycolysis. Measurement of G6PDH and 6PGDH activities revealed that the enzymatic activities themselves are not up-regulated under photomixotrophic conditions (Fig. 6), which is consistent with the previous reports (Knowles and Plaxton, 2003; Singh and Sherman, 2005; Kahlon *et al*., 2006). It is likely that the abundant supply of substrates under photomixotrophic conditions leads to the enhancement of sugar catabolism. Judging from 1.5-fold higher oxygen consumption rate in photomixotrophically grown cells than that in photoautotrophically grown cells (Fig. 7B), the respiratory electron transport seems to be also activated under photomixotrophic conditions.

On the other hand, the carbon flow through the Calvin cycle seems to decrease

under photomixotrophic conditions, judging from the decrease in the Calvin cycle intermediates (Fig. 3) and photosynthetic activity (Fig. 7A). This indicates that the restriction of photosynthesis is one of the strategies of *Synechocystis* sp. PCC 6803 to adapt to photomixotrophic condition. Amount of RuBP, 3PGA, PEP and pyruvate significantly decreased upon the addition of glucose in contrast to the increase of Ru5P and GA3P (Fig. 3). Phosphoribulokinase (PRK) and glyceraldehyde-3-phosphate dehydrogenase (GAPDH) catalyzing the conversions of Ru5P and GA3P to RuBP and 3PGA, respectively, are known to be key enzymes for the regulation of carbon flow between the Calvin cycle and the OPP pathway (Wedel and Soll, 1998). Increase of substrates and decrease of products of these enzymes under photomixotrophic conditions are probably caused by the repression of the activities of PRK and GAPDH. In *Synechococcus* sp. PCC 7942 cultured under a 12 h-light/12h-dark cycle, the down-regulation of the Calvin cycle during the dark period was shown to be attained through the complex formation of GAPDH, PRK and a small protein named CP12 in response to the decrease in the NADP(H)/NAD(H) ratio (Tamoi *et al*., 2005). It is reasonable to assume that this inhibitory mechanism works in photomixotrophically grown *Synechocystis*, because we observed significant decrease of the NADP(H)/NAD(H) ratio by the addition of glucose, from 2.3 to 1.4 in the wild-type

cells. Upon the shift to photomixotrophic conditions, the extent of decrease in the amount of the Calvin cycle intermediates such as RuBP and 3PGA (Fig. 3) was much larger than that in photosynthetic activity (Fig. 7A). It is possible that these metabolites hardly accumulate under photomixotrophic conditions probably due to the increased metabolic flux to the OPP pathway and to TCA cycle.

Among metabolites in TCA cycle, the amount of malate, fumarate, and isocitrate increased under photomixotrophic conditions, whereas that of succinate and 2-OG decreased (Fig. 4A). In cyanobacteria lacking both 2-oxoglutarate dehydrogenase and succinyl-CoA synthetase activities (Pearce *et al*., 1969), succinate and 2-OG are terminal metabolites of TCA cycle and serve as a precursor of various biosynthetic reactions. Succinate is a substrate for succinate dehydrogenase (SDH) that is a major component of cyanobacterial respiratory electron transport chain (Cooley and Vermaas, 2001). On the other hand, 2-OG serves as a carbon skeleton required for nitrogen assimilation and also works as a regulatory metabolite involved in coordination between carbon and nitrogen metabolism (Muro-Pastor *et al*., 2001). Enhancemenet of SDH activity and nitrogen assimilation may be the cause of decrease in these metabolites under photomixotrophic conditions.

The difference in metabolic processes between the wild-type and ΔpmgA mutant cells under photomixotrophic conditions

Growth of Δ*pmgA* mutant is severely inhibited after 24 h of incubation under photomixotrophic conditions, although the wild-type cells can grow normally. CE/MS analysis and measurement of enzymatic-, photosynthetic- and respiratory-activities suggested that Δ*pmgA* mutant has defect in the coordination of anabolic and catabolic activities, leading to the metabolic imbalance and the growth inhibition under photomixotrophic conditions.

The low amount of 6PG, Ru5P, R5P (Fig. 3) and NADPH (Fig. 5) together with the low activities of G6PDH and 6PGDH (Fig. 6) observed in photomixotrophically-grown Δ*pmgA* mutant indicated the decreased carbon flow to the OPP pathway. The respiratory activity of Δ*pmgA* mutant cells was not up-regulated under photomixotrophic conditions (Fig. 7B), which is likely due to the diminished amount of NADPH. Furthermore, the low respiratory activity in the mutant may result in decreased rate of ATP synthesis through oxidative phosphorylation (Fig. 5).

The decrease in photosynthetic activity upon the shift to photomixotrophic conditions was observed in Δ*pmgA* mutant as well as in the wild type (Fig. 7A). Amounts of RuBP, 3PGA, PEP and pyruvate largely decreased in the both strains (Fig.

3), suggesting that inhibitory mechanism of PRK and GAPDH normally operates in the mutant. However, Δ*pmgA* mutant still showed higher rate of photosynthetic activity than the wild-type under photomixotrophic conditions (Fig. 7A). Active CO_2 fixation together with the slowdown of the regeneration of RuBP, the substrate of CO_2 fixation, is likely to cause the decrease in RuBP level in the mutant (Fig. 3).

The most notable difference between the wild-type and Δ*pmgA* mutant was seen in the isocitrate content under photomixotrophic conditions. Aberrant accumulation of isocitrate was observed in Δ*pmgA* mutant cells within 6 h after the addition of glucose (Fig. 4B). The conversion of citrate to isocitrate catalyzed by aconitase and that of isocitrate to 2-OG catalyzed by $NADP^+$-ICDH were normally operated in Δ*pmgA* mutant (Fig. 6). Perhaps higher activity of the Calvin cycle in Δ*pmgA* mutant brings about the excess supply of carbon materials, leading to the isocitrate accumulation. Sakuragi *et al*. (2006) reported that Δ*pmgA* mutant accumulated twice as much total sugar as the wild type under photoautotrophic and photomixotrophic conditions. This observation also indicates the excess carbon flow within Δ*pmgA* mutant cells.

It is of note that low enzymatic activities in the OPP pathway (Fig. 6) and high photosynthetic activity (Fig. 7A) can be observed in the mutant not only under photomixotrophic but also under photoautotrophic conditions. In spite of these defects,

amounts of metabolites in the mutant were not so much different from those in the wild type under photoautotrophic conditions. The low enzymatic activity in the mutant could not be rate-limiting under photoautotrophic conditions, since the carbon flow to the OPP pathway is largely restricted due to low availability of substrates. Without conflicting with the activity of the OPP pathway, higher activity of the Calvin cycle in the mutant could bring about higher growth rate under photoautotrophic conditions (Hihara *et al*., 1998). Apparently, a delicate balancing between anabolic and catabolic activities is indispensable for growth specifically under photomixotrophic conditions where both light and glucose are available. PmgA is likely to be involved in this regulation by partitioning of the carbon flow between the Calvin cycle and the OPP pathway.

Acknowledgments

This work was supported by a Grant-in-Aid for Young Scientists of the Japan Society for the Promotion of Science and a grant from the Ministry of Agriculture, Forestry and Fishery, Japan and CREST, JST, Japan

References

Cooley JW, Vermaas WFJ. 2001. Succinate dehydrogenase and other respiratory pathways in thylakoid membranes of *Synechocystis* sp.strain PCC 6803: Capacity comparisons and physiological function. *Journal of Bacteriology* **183,** 4251-4258.

Gill RT, Katsoulakis E, Schmitt W, Taroncher-Oldenburg G, Misra J, Stephanopoulos G. 2002. Genome-wide dynamic transcriptional profiling of the light-to-dark transition in *Synechocystis* sp. strain PCC 6803. *Journal of Bacteriology* **184,** 3671-3681.

Herranen M, Battchikova N, Zhang P, Graf A, Sirpio S, Paakkarinen V, Aro EM. 2004. Towards functional proteomics of membrane protein complexes in *Synechocystis* sp. PCC 6803. *Plant Physiology* **134,** 470-481.

Hihara Y, Ikeuchi M. 1997. Mutation in a novel gene required for photomixotrophic growth leads to enhanced photoautotrophic growth of *Synechocystis* sp. PCC 6803. *Photosynthesis Research* **53,** 243-252.

Hihara Y, Sonoike K, Ikeuchi M. 1998. A novel gene, *pmgA*, specifically regulates photosystem stoichiometry in the cyanobacterium *Synechocystis* sp. PCC 6803 in response to high light. *Plant Physiology* **117,** 1205-1216.

Kahlon S, Beeri K, Ohkawa H, Hihara Y, Murik O, Suzuki I, Ogawa T, Kaplan A.

2006. A putative sensor kinase, Hik31, is involved in the response of *Synechocystis* sp. strain PCC 6803 to the presence of glucose. *Microbiology* **152,** 647-655.

Knowles VL, Plaxton WC. 2003. From genome to enzyme: Analysis of key glycolytic and oxidative pentose-phosphate pathway enzymes in the cyanobacterium *Synechocystis* sp. PCC 6803. *Plant and Cell Physiology* **44,** 758-763.

Kurian D, Jansen T, Maenpaa P. 2006. Proteomic analysis of heterotrophy in *Synechocystis* sp. PCC 6803. *Proteomics* **6,** 1483-1494.

Muro-Pastor MI, Reyes JC, Florencio FJ. 2001. Cyanobacteria perceive nitrogen status by sensing intracellular 2-oxoglutarate levels. *Journal of Biological Chemistry* **276,** 38320-38328.

Pearce J, Leach CK, Carr NG. 1969. The incomplete tricarboxylic acid cycle in the blue-green alga *Anabaena variabilis*. *Journal of General Microbiology* **55,** 371-378.

Pelroy RA, Rippka R, Stanier RY. 1972. Metabolism of glucose by unicellular blue-green algae. *Archiv für Mikrobiologie* **87,** 303-322.

Rippka R, Deruelles J, Waterbury J-B, Herdman M, Stanier RY. 1979. Genetic assignments, strain histories and properties of pure cultures of cyanobacteria. *Journal of General Microbiology* **111,** 1-61.

Sakuragi Y, Maeda H, DellaPenna D, Bryant DA. 2006. α-tocopherol plays a role in

photosynthesis and macronutrient homeostasis of the cyanobacterium *Synechocystis* sp. PCC 6803 that is independent of its antioxidant function. *Plant Physiology* **141,** 508-521.

Sato S, Soga T, Nishioka T, Tomita M. 2004. Simultaneous determination of the main metabolites in rice leaves using capillary electrophoresis mass spectrometry and capillary electrophoresis diode array detection. *Plant Journal* **40,** 151-163.

Singh AK, Sherman LA. 2005. Pleiotropic effect of a histidine kinase on carbohydrate metabolism in *Synechocystis* sp. strain PCC 6803 and its requirement for heterotrophic growth. *Journal of Bacteriology* **187,** 2368-2376.

Smith AJ. 1982. Modes of cyanobacterial carbon metabolism. In: Carr NG, Whitton BA, eds. *The biology of cyanobacteria*, Berkeley, CA: University of California Press, 47-85.

Soga T, Ueno Y, Naraoka H, Ohashi Y, Tomita M, Nishioka T. 2002. Simultaneous determination of anionic intermediates for *Bacillus subtilis* metabolic pathways by capillary electrophoresis electrospray ionization mass spectrometry. *Analytical Chemistry* **74,** 2233-2239.

Stal LJ, Moezelaar R. 1997. Fermentation in cyanobacteria. *FEMS Microbiology Reviews* **21,** 179-211.

Takahashi H, Hayashi M, Goto F, Sato S, Soga S, Nishioka T, Tomita M, Kawai-Yamada M, Uchimiya H. 2006*a*. Evaluation of metabolic alteration in transgenic rice overexpressing dihydroflavonol-4-reductase. *Annals of Botany* **98,** 819-825.

Takahashi H, Watanabe A, Tanaka A, Hashida S-N, Kawai-Yamada M, Sonoike K, Uchimiya H. 2006*b*. Chloroplast NAD kinase is essential for energy transduction through the xanthophyll cycle in photosynthesis. *Plant and Cell Physiology* **47,** 1678-1682.

Tamoi M, Miyazaki T, Fukamizo T, Shigeoka S. 2005. The calvin cycle in cyaobacteria is regulated by CP12 via the NAD(H)/NADP(H) ratio under light/dark conditions. *Plant Journal* **42,** 504-513.

Trentham DR, McMurray CH, Pogson CI. 1969. The active chemical state of D-glyceraldehyde 3-phosphate in its reactions with D-glyceraldehyde 3-phosphate dehydrogenase, aldolase and triose phosphate isomerase. *Biochemical Journal* **114**, 19-24.

Wedel N, Soll J. 1998. Evolutionary conserved light regulation of Calvin cycle activity by NADPH-mediated reversible phosphoribulokinase/CP12/ glyceraldehyde-3-phosphate dehydrogenase complex dissociation. *Proceedings of*

the National Academy of Sciences, USA **95,** 9699-9704.

Yang C, Hua Q, Shimizu K. 2002*a*. Integration of the information from gene expression and metabolic fluxes for the analysis of the regulatory mechanisms in *Synechocystis*. *Applied Microbiology and Biotechnology* **58,** 813-822.

Yang C, Hua Q, Shimizu K. 2002*b*. Metabolic flux analysis in *Synechocystis* using isotope distribution from ^{13}C-labeled glucose. *Metabolic Engineering* **4,** 202-216.

Yang C, Hua Q, Shimizu K. 2002*c*. Quantitative analysis of intracellular metabolic fluxes using GC-MS and two-dimensional NMR spectroscopy. *Journal of Bioscience and Bioengineering* **93**, 78-87.

Figure Legends

Fig. 1 Growth curve of the wild-type (open circle) and Δ*pmgA* (closed circle) cells in liquid BG-11 medium supplemented with 5 mM glucose. Cultures grown at 50 μmol photons $m^{-2}s^{-1}$ were supplemented with glucose at time 0, and diluted every 24 h to avoid the self shading of cells.

Fig. 2 The central metabolic pathway of *Synechocystis* sp. PCC 6803 in the integration of metabolites described in this study. Thick arrows indicate the direction of

the metabolic flow of the Calvin cycle.

Fig. 3 Amounts of metabolites in glycolysis, the OPP pathway and the Calvin cycle. Wild-type and Δ*pmgA* mutant were grown photoautotrophically (white bar) or photomixotrophically (black bar) for 24 h, and then metabolite contents were quantified. Each value represents the means ± SD of three independent experiments (nmol g^{-1} fresh weight).

Fig. 4 Amounts of metabolites in the TCA cycle. (A) Comparison of metabolite contents in wild-type and Δ*pmgA* mutant grown photoautotrophically (white bar) or photomixotrophically (black bar) for 24 h. Each value represents the means ± SD of three independent experiments (nmol g^{-1} fresh weight). (B) The time course of isocitrate (ICA) accumulation after the addition of glucose. Electropherograms (m/z 191) were obtained every 6 h after glucose addition using CE/MS and signal abundances were normalized to fresh weight and internal standard level.

Fig. 5 Amounts of adenine- and pyridine-nucleotides. Wild-type and Δ*pmgA* mutant were grown photoautotrophically (white bar) or photomixotrophically (black bar) for 24

h, and then metabolite contents were quantified. Each value represents the means ± SD of three independent experiments (nmol g^{-1} fresh weight).

Fig. 6 Change in activities of G6PDH, 6PGDH, aconitase and ICDH in the wild-type (open circle) and Δ*pmgA* (closed circle) cells upon the shift from photoautotrophic- to photomixotrophic conditions. Cultures grown at 50 μmol photons $m^{-2}s^{-1}$ were supplemented with 5 mM glucose at time 0. Samples were taken at the indicated time points, and enzymatic activities in cell extracts were determined as described in Materials and Methods. Data are the means ± SD of three independent experiments.

Fig. 7 Photosynthetic (A) and respiratory (B) activities of the wild-type and Δ*pmgA* cells incubated under photoautotrophic- or photomixotrophic-conditions for 24 h. Photosynthetic activity was measured as oxygen evolution supported by 2 mM $NaHCO_3$ at 50 μmol photons m^{-2} s^{-1}. Respiratory activity was measured as oxygen consumption in the presence of 5 mM glucose in the dark. Data are the means ± SD of three independent experiments.

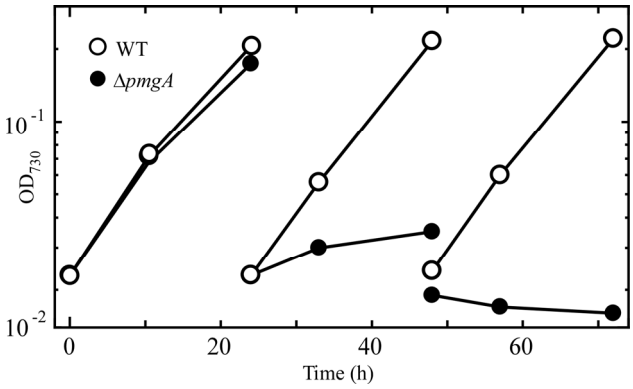

Fig. 1

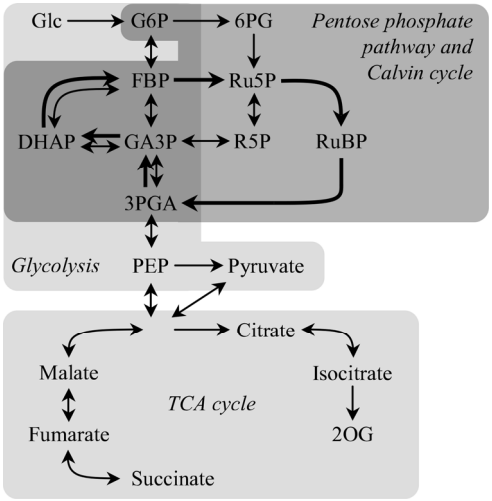
Glc
G6P
6PG
Pentose phosphate pathway and Calvin cycle
FBP
Ru5P
DHAP
GA3P
R5P
RuBP
3PGA
Glycolysis
PEP
Pyruvate
Citrate
Malate
Isocitrate
TCA cycle
Fumarate
2OG
Succinate

Fig. 2

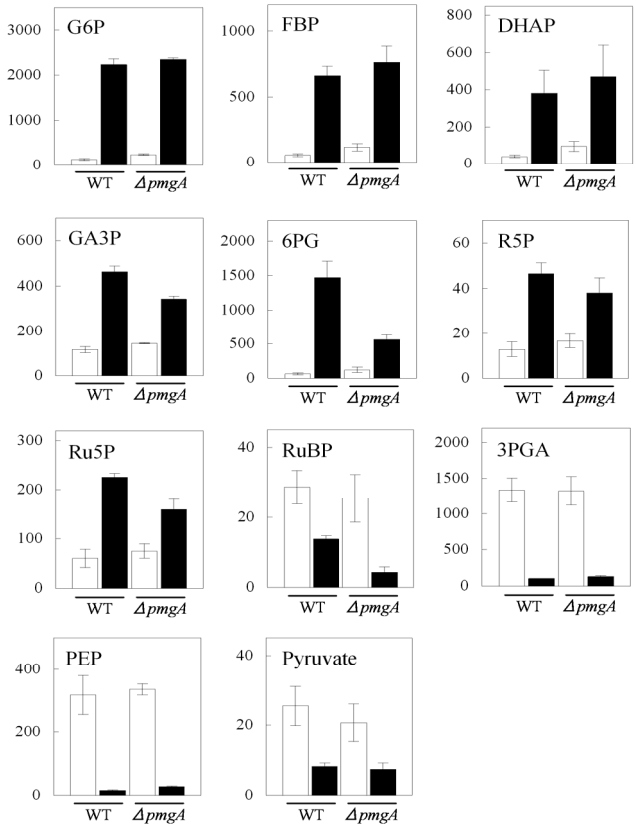
G6P
3000
2000
1000
0
WT
ΔpmgA
FBP
1000
500
0
WT
ΔpmgA
DHAP
800
600
400
200
0
WT
ΔpmgA
GA3P
600
400
200
0
WT
ΔpmgA
6PG
2000
1500
1000
500
0
WT
ΔpmgA
R5P
60
40
20
0
WT
ΔpmgA
Ru5P
300
200
100
0
WT
ΔpmgA
RuBP
40
20
0
WT
ΔpmgA
3PGA
2000
1500
1000
500
0
WT
ΔpmgA
PEP
400
200
0
WT
ΔpmgA
Pyruvate
40
20
0
WT
ΔpmgA

Fig. 3

(A)

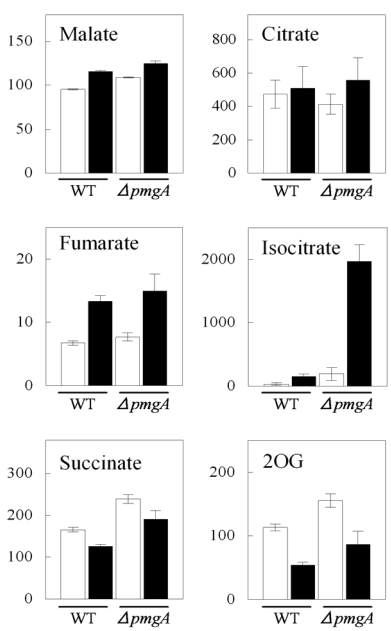
Malate
Citrate
Fumarate
Isocitrate
Succinate
2OG
WT
ΔpmgA

(B)

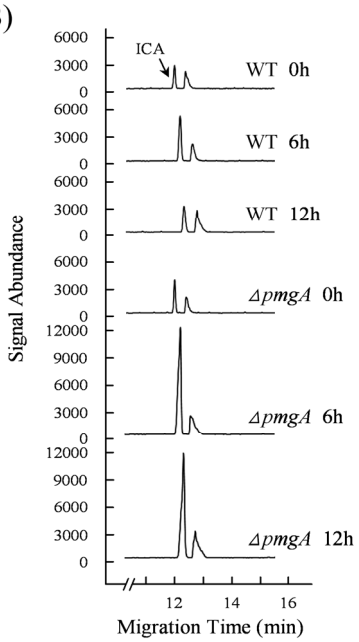
ICA
WT 0h
WT 6h
WT 12h
ΔpmgA 0h
ΔpmgA 6h
ΔpmgA 12h
Signal Abundance
Migration Time (min)

Fig. 4

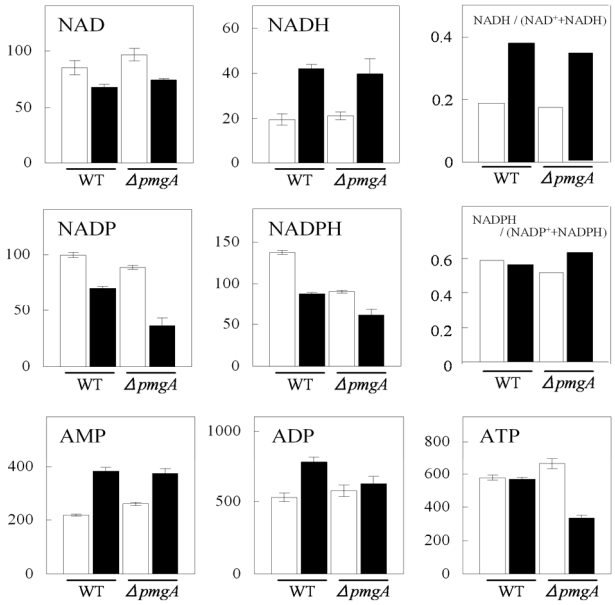
NAD
NADH
NADH / (NAD+NADH)
NADP
NADPH
NADPH / (NADP+NADPH)
AMP
ADP
ATP
WT
ΔpmgA

Fig. 5

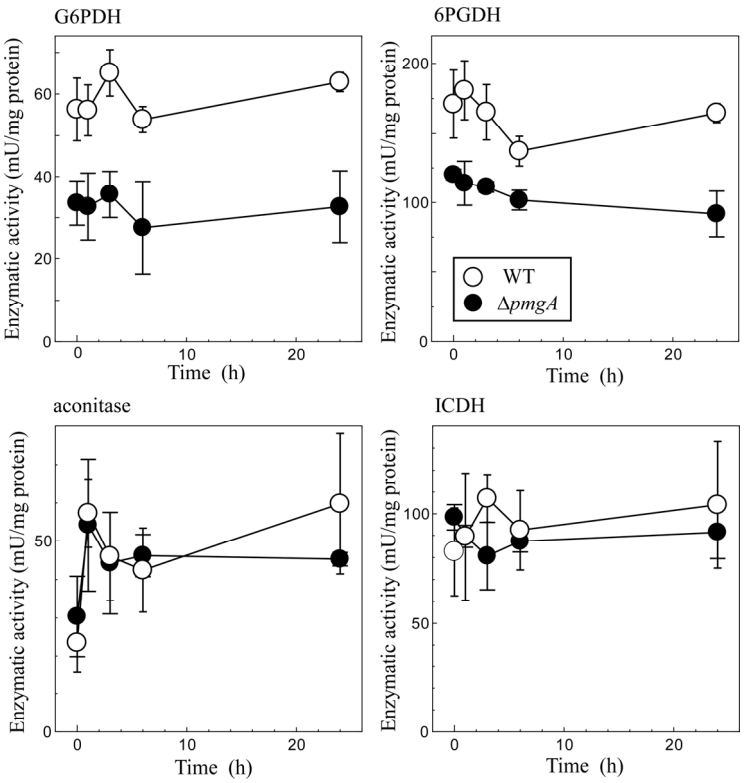
G6PDH
6PGDH
aconitase
ICDH
Enzymatic activity (mU/mg protein)
Time (h)
WT
ΔpmgA

Fig. 6

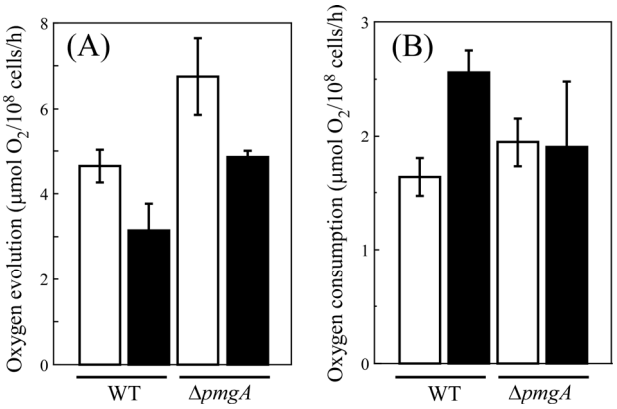
(A)
Oxygen evolution (μmol O_2/10^8 cells/h)
0
2
4
6
8
WT
ΔpmgA
(B)
Oxygen consumption (μmol O_2/10^8 cells/h)
0
1
2
3
WT
ΔpmgA

Fig. 7